NASA-CR-177924
19850014788

NASA Contractor Report 177924

STRESS INTENSITY FACTOR IN A TAPERED SPECIMEN

Liu Xue-Hui and F. Erdogan

LEHIGH UNIVERSITY
Bethlehem, Pennsylvania

Grant NGR 39-007-011
April 1985

National Aeronautics and
Space Administration

Langley Research Center
Hampton, Virginia 23665

STRESS INTENSITY FACTOR IN A TAPERED SPECIMEN

by

Liu Xue-Hui* and F. Erdogan
Lehigh University, Bethlehem, PA 18015

Abstract

In this paper the general problem of a tapered specimen containing an edge crack is formulated in terms of a system of singular integral equations. The equations are solved and the stress intensity factor is calculated for a "compact" and for a "slender" tapered specimen, the latter simulating the double cantilever beam. The results are obtained primarily for a pair of concentrated forces and for crack surface wedge forces. The stress intensity factors are also obtained for a long strip under uniform tension which contains inclined edge cracks.

1. Introduction

The main objective of this paper is to provide a solution for a tapered specimen containing an edge crack by using an integral equation technique. The geometry of the specimen is shown in Fig. 1 where the dimensions H, B, ℓ, m, n, and θ are arbitrary. By choosing the relative dimensions properly one may simulate either the tapered compact tension specimen (Fig. 1) or the tapered double cantilever beam specimen (Fig. 2). Even though the results are given only for two types of loading shown in Figures (1a) and (1b), the formulation of the problem is quite general and any arbitrary loading on the crack surfaces or on the inclined boundaries, for example, can easily be taken into account. Of course, the problem can also be solved by using a finite element method. Because of its practical importance the rectangular specimen having an edge crack has been studied rather widely (see, for example, [1] and the articles by Bowie, Isida, and Wilson in [2]). The general problem was also discussed in a recent article [3].

*Current address: Institute of Structure Strength, Northwestern Polytechnical University, Xian, Shaanxi, The People's Republic of China

2. Formulation of the Problem

We will first consider the general crack problem for an infinite strip described in Fig. 3. It will be assumed that y=0 is a plane of symmetry and the location (m,n) of the concentrated force P and the crack surface tractions are arbitrary. For the purpose of deriving the integral equations one may express the stress state at a point (x,y) in the strip as follows:

$$\sigma_{ij}(x,y) = \sigma_{1ij}(x,y) + \sigma_{2ij}(x,y) + \sigma_{3ij}(x,y) + \sigma_{4ij}(x,y) + \sigma_{5ij}(x,y) , \qquad (i,j=x,y) \qquad (1)$$

where the stress components σ_{1ij} are associated with an infinite plane containing a crack along (y=0, a<x<b), σ_{2ij} and σ_{3ij} are associated with a plane having a crack along (c<r<d, θ) and (c<r<d, $-\theta$), respectively, σ_{4ij} relate to an infinite plane without any cracks under concentrated forces P at x=m, y=$\mp$n, and σ_{5ij} are associated with an infinite strip. The total stress state σ_{ij} must satisfy the following boundary conditions (Fig. 3):

$$\sigma_{xx}(0,y) = 0, \ \sigma_{xy}(0,y) = 0, \ (0\leq y<\infty) , \qquad (2)$$

$$\sigma_{xx}(H,y) = 0, \ \sigma_{xy}(H,y) = 0, \ (0\leq y<\infty) , \qquad (3)$$

$$\sigma_{xy}(x,0) = 0, \ (0<x<H) , \qquad (4)$$

$$\sigma_{yy}(x,0) = p_1(x), \ (a<x<b) , \qquad (5)$$

$$\sigma_{\theta\theta}(r,\theta) = p_2(r), \ (c<r<d) , \qquad (6)$$

$$\sigma_{r\theta}(r,\theta) = p_3(r), \ (c<r<d) , \qquad (7)$$

where p_1, p_2 and p_3 are known functions and where it is assumed that because of symmetry only one half (y>0) of the domain needs to be considered.

We now define the following unknown functions:

$$g_1(x) = \frac{\partial}{\partial x}[u_y(x,+0)-u_y(x,-0)], \ (a<x<b) , \qquad (8)$$

$$g_2(r) = \frac{\partial}{\partial r}[u_\theta(r,\theta+0)-u_\theta(r,\theta-0)], \ (c<r<d) , \qquad (9)$$

$$g_3(r) = \frac{\partial}{\partial r}[u_r(r,\theta+0)-u_r(r,\theta-0)],\ (c<r<d)\ , \tag{10}$$

$$g_4(r) = \frac{\partial}{\partial r}[u_\theta(r,-\theta+0)-u_\theta(r,-\theta-0)],\ (c<r<d)\ , \tag{11}$$

$$g_5(r) = \frac{\partial}{\partial r}[u_r(r,-\theta+0)-u_r(r,-\theta-0)],\ (c<r<d) \tag{12}$$

where u_x, u_y or u_r, u_θ are the components of the displacement vector referred to x,y or r,θ coordinates, respectively (Fig. 3). The stress state associated with an infinite plane containing a symmetrically loaded crack on the x axis may then be expressed as

$$\sigma_{1ij}(x,y) = \int_a^b G_{ij}(x,y,t,0)g_1(t)dt\ ,\ (i,j=x,y) \tag{13}$$

where the kernels G_{ij} are given in Appendix A. The stresses associated with edge dislocations of densities g_2 and g_3 distributed along (c<r<d, θ = constant) are given by

$$\sigma_{2ij}(x,y) = \int_c^d G_{ij}(x,y,x_o,y_o)[g_2(r_o)\cos\theta+g_3(r_o)\sin\theta]dr_o + \int_c^d H_{ij}(x,y,x_o,y_o)[g_3(r_o)\cos\theta-g_2(r_o)\sin\theta]dr_o\ ,\ (i,j=x,y)\ , \tag{14}$$

where $G_{ij}(x,y,x_o,y_o)$ and $H_{ij}(x,y,x_o,y_o)$, (i,j=x,y) are again given in Appendix A, and

$$x_o = r_o\cos\theta\ ,\ y_o = B + r_o\sin\theta\ . \tag{15}$$

Similarly, for the crack lying along (c<r<d, -θ) we have

$$\sigma_{3ij}(x,y) = \int_c^d G_{ij}(x,y,x_o,y_o)[g_4(r_o)\cos\theta-g_5(r_o)\sin\theta]dr_o + \int_c^d H_{ij}(x,y,x_o,y_o)[g_5(r_o)\cos\theta+g_4(r_o)\sin\theta]dr_o,\ (i,j=x,y), \tag{16}$$

$$x_o = r_o\cos\theta \ , \ y_o = -B-r_o\sin\theta \ . \tag{17}$$

The stresses due to a pair of concentrated forces P and -P (per unit thickness) are given by (Fig. 3)

$$\sigma_{4ij}(x,y) = P\ Q_{ij}(x,y,m,n) \ , \ (i,j=x,y) \tag{18}$$

where the functions Q_{ij} are given in Appendix B.

Finally, by using Fourier transforms and the symmetry of the problem, the stresses in an infinite strip $0<x<H$, $-\infty<y<\infty$ may be expressed as

$$\begin{aligned}
\sigma_{5xx}(x,y) &= -\frac{4\mu}{\pi}\int_o^\infty \{[\alpha(A_1+xA_2)+\tfrac{1+\kappa}{2}A_2]e^{-\alpha x} \\
&\quad + [\alpha(A_3+xA_4)-\tfrac{1+\kappa}{2}A_4]e^{\alpha x}\}\cos\alpha y\,d\alpha \ , \\
\sigma_{5yy}(x,y) &= \frac{4\mu}{\pi}\int_o^\infty \{[\alpha(A_1+xA_2)+\tfrac{\kappa-3}{2}A_2]e^{-\alpha x} \\
&\quad + [\alpha(A_3+xA_4)-\tfrac{\kappa-3}{2}A_4]e^{\alpha x}\}\cos\alpha y\,d\alpha \ , \\
\sigma_{5xy}(x,y) &= -\frac{4\mu}{\pi}\int_o^\infty \{[\alpha(A_1+xA_2)+\tfrac{\kappa-1}{2}A_2]e^{-\alpha x} \\
&\quad - [\alpha(A_3+xA_4)-\tfrac{\kappa-1}{2}A_4]e^{\alpha x}\}\sin\alpha y\,d\alpha \ ,
\end{aligned} \tag{19a-c}$$

where $A_1,\ldots,A_4$ are unknown functions of α.

If we now substitute from (13)-(19) into (1), use the homogeneous boundary conditions (2) and (3), invert the Fourier transforms and evaluate the resulting infinite integrals, we obtain the unknown functions $A_1,\ldots,A_4$ in the following form:

$$\begin{aligned}
A_i(\alpha) &= \sum_{k=1}^{3}\int_{a_k}^{b_k} B_{ik}(\alpha,t)g_k(t)dt + PC_i(\alpha) \ , \ (i=1,\ldots,4, \\
&\qquad a_1=a,\ b_1=b,\ a_k=c,\ b_k=d,\ k=2,3) \ ,
\end{aligned} \tag{20}$$

where the symmetry properties

$$u_\theta(r,-\theta+0)-u_\theta(r,-\theta-0) = u_\theta(r,\theta+0)-u_\theta(r,\theta-0),$$

$$u_r(r,-\theta+0)-u_r(r,-\theta-0) = -[u_r(r,\theta+0)-u_r(r,\theta-0)] \qquad (21a,b)$$

have been used. The explicit expressions of A_i may be found in Appendix C.

We now observe that the boundary condition (4) is satisfied by the assumed symmetry and from (9)-(12) and (21) we have

$$g_4(r) = g_2(r) \ , \ g_5(r) = -g_3(r) \ . \qquad (22)$$

The three remaining boundary conditions (5)-(7) may then be used to determine the unknown functions g_1, g_2 and g_3. Thus, by substituting from (13)-(20) into (5)-(7) and by using (22) we obtain the following system of integral equations to determine g_1, g_2 and g_3

$$\sum_{j=1}^{3} \int_{a_j}^{b_j} h_{ij}(s,t)g_j(t)dt = p_i(s) + P\, h_i(s) \ , \ (i=1,2,3; \quad a_1=a<s=x<b=b_1, \ a_k=c<s=r<d=b_k, \ k=1,2) \ , \qquad (23)$$

where h_{ij}, $(i,j=1,2,3)$ and h_i, $(i=1,2,3)$ are known functions and may be expressed in terms of infinite integrals of the following form by using the information given in the appendices A, B and C:

$$h_{ij}(s,t) = \int_0^\infty K_{ij}(s,t,\alpha)d\alpha \ , \ (i,j=1,2,3) \ , \qquad (24)$$

$$h_i(s) = \int_0^\infty K_i(s,\alpha)d\alpha \ , \ (i=1,2,3) \ . \qquad (25)$$

For the crack problem shown in Fig. 3, by separating singular part of the kernels h_{ij} through an asymptotic analysis, it can be shown that the main diagonal elements of h_{ij} have Cauchy type singularities. That is, for $\alpha\to\infty$ if we let

$$K_{ij}(s,t,\alpha) \to K_{ij\infty}(s,t,\alpha) \tag{26}$$

we find

$$\int_0^\infty K_{ii\infty}(s,t,\alpha)d\alpha = \frac{2\mu}{\pi(1+\kappa)} \frac{1}{t-s} \ , \ (i=1,2,3) \tag{27}$$

and the kernels h_{ij} may be expressed as

$$h_{ij}(s,t) = \frac{2\mu}{\pi(1+\kappa)} \frac{\delta_{ij}}{t-s} + k_{ij}(s,t) \ , \ (i,j=1,2,3) \tag{28}$$

where the functions k_{ij} are bounded within the closed interval $a_j \leq (s,t) \leq b_j$, $(j=1,2,3)$. From the definitions given by (8)-(10) and from Fig. 3 it is clear that the density functions $g_j(t)$, $(j=1,2,3)$ must satisfy

$$\int_a^b g_1(t)dt = 0 \ , \ \int_c^d g_k(t)dt = 0 \ , \ (k=2,3) \ . \tag{29}$$

Referring to, for example, [4], it is known that the solution of the system of singular integral equations may be expressed as

$$g_1(t) = \frac{F_1(t)}{\sqrt{(t-a)(b-t)}} \ , \ (a<t<b) \ , \tag{30}$$

$$g_k(t) = \frac{F_k(t)}{\sqrt{(t-c)(d-t)}} \ , \ (k=1,2; \ c<t<d) \ . \tag{31}$$

The Modes I and II crack tip stress intensity factors may then be defined by and evaluated from the following relations:

$$k_1(a) = \lim_{x\to a} \sqrt{2(a-x)}\, \sigma_{yy}(x,0) = \frac{2\mu}{1+\kappa} \lim_{x\to a} \sqrt{2(x-a)}\, g_1(x),$$

$$k_1(b) = \lim_{x\to b} \sqrt{2(x-b)}\, \sigma_{yy}(x,0) = -\frac{2\mu}{1+\kappa} \lim_{x\to b} \sqrt{2(b-x)}\, g_1(x) \ , \tag{32 a,b}$$

$$k_1(c) = \lim_{r\to c} \sqrt{2(c-r)}\, \sigma_{\theta\theta}(r,\theta) = \frac{2\mu}{1+\kappa} \lim_{r\to c} \sqrt{2(r-c)}\, g_2(r) \ ,$$

$$k_2(c) = \lim_{r\to c} \sqrt{2(c-r)}\, \sigma_{r\theta}(r,\theta) = \frac{2\mu}{1+\kappa} \lim_{r\to c} \sqrt{2(r-c)}\, g_3(r) \ , \tag{33 a,b}$$

$$k_1(d) = \lim_{r\to d} \sqrt{2(r-d)}\, \sigma_{\theta\theta}(r,\theta) = -\frac{2\mu}{1+\kappa} \lim_{r\to d} \sqrt{2(d-r)}\, g_2(r) \ ,$$

$$k_2(d) = \lim_{r\to d} \sqrt{2(r-d)}\, \sigma_{r\theta}(r,\theta) = -\frac{2\mu}{1+\kappa} \lim_{r\to d} \sqrt{2(d-r)}\, g_3(r) \ . \qquad (34\ a,b)$$

The functions $h_i(s)$, (i=1,2,3) and the kernels $h_{ij}(s,t)$, (i,j=1,2,3) may be evaluated in terms of G_{ij}, H_{ij}, Q_{ij}, (i,j=x,y), and A_i, (i=1,...,4) in a straightforward manner. However, the manipulations and the resulting expressions are quite lengthy and will not be reproduced in this paper.

We also note that in obtaining the integral equations from the crack surface boundary conditions (6) and (7), the stress state $\sigma_{ij}(x,y)$, (i,j= x,y) as given by (1) is substituted into

$$p_2(r) = \sigma_{\theta\theta}(r,\theta) = \sigma_{xx}(x,y)\sin^2\theta + \sigma_{yy}(x,y)\cos^2\theta - 2\sigma_{xy}(x,y)\sin\theta\cos\theta \ ,$$

$$p_3(r) = \sigma_{r\theta}(r,\theta) = [\sigma_{yy}(x,y)-\sigma_{xx}(x,y)]\sin\theta\cos\theta + \sigma_{xy}(x,y)(\cos^2\theta-\sin^2\theta) \ ,$$

$$x = r\cos\theta \ , \ y = B + r\sin\theta \ , \ (\theta = \text{constant}, \ c<r<d) \ . \qquad (35\ a\text{-}d)$$

For the case of "edge" cracks, i.e., for a=0 or c=0, the asymptotic analysis would show that the singular parts of the kernels $h_{ij}(s,t)$ are generalized Cauchy kernels. That is, as shown, for example, in [5] the singular parts contain, in addition to the standard Cauchy kernels, terms that become unbounded as the variables s and t approach zero simultaneously and as a consequence at the end point t=0 the density functions $g_i(t)$, (i=1,2,3) become bounded (see, also [3]). The integral equations were solved by using the technique described, for example, in [6] (see also, [5]).

3. Numerical Results

The first numerical example considered is described by the insert in Fig. 4, namely a long strip containing two symmetrically located inclined edge cracks. Rather extensive results for parallel cracks may be found in [3]. For a given B/H ratio (of 0.2) the normalized stress intensity factors are given in Table 1. In this example, the relative crack length ℓ and the angle θ are the variables. Table 1 shows the results for a uniform tension

$\sigma_{yy}=\sigma_o$ away from the crack region. In this case the crack surface tractions for the perturbation problem are the input functions in the integral equations (23) and are given by

$$p_2(r) = -\sigma_o\cos^2\theta,\ p_3(r) = -\sigma_o\sin\theta\cos\theta\ . \tag{36}$$

The special case of this problem for $\theta=0$ was studied in [3] and are also calculated here for comparison. It may be observed that for small values of θ $k_2(d)$ is negative and, as pointed out in [3], would force the cracks to grow away from each other. However, for relatively large values of θ $k_2(d)$ becomes positive. This means that for such angles the cracks tend to grow toward each other or, they tend to orient themselves more nearly perpendicular to the direction of the external load. This, of course, is the physically expected result. Theoretically, if the Mode II stress intensity factor $k_2(d)$ is zero, momentarily the crack would be expected to grow in its current plane. Table 1 implies that for a given crack length ℓ/H the value of $\theta=\theta_o$ corresponding to $k_2(d)=0$ can be calculated. For B/H = 0.2 the calculated values of θ_o are shown in Fig. 4.

Table 2 shows the results for three edge cracks of equal length in a long strip under uniform tension σ_o away from the crack region. In this case too the results for $\theta=0$ agree with those given in [3].

Tables 3-5 show the results for a tapered "compact" specimen containing an edge crack ($a=0$, $b=\ell$). The stress intensity factor given in Table 3 correspond to a uniformly pressurized crack shown in Fig. (1a) for B/H = 0.2 and B/H = 0.48. Tables 4 and 5 give the stress intensity factors for a pair of concentrated forces and crack surface wedge forces, respectively.

The stress intensity factor for a "slender" tapered specimen (or the tapered double cantilever beam specimen) described in Fig. 2 is given in Fig. 5. The figure indicates that for B/H=0.1 one could have a "constant k" regime only for $\theta=30°$ and $0.15<\ell/H<0.4$. For the double cantilever beam specimen an approximate value of the stress intensity factor may also be obtained by using the following energy balance relation (Fig. 2):

$$\frac{\partial}{\partial L}(U-V) = \frac{\pi k_1^2(b)}{E'}\ , \tag{37}$$

where L is the length of the "beam" (Fig. 2), U is the work of the external forces P, V is the strain energy, $E'=E$ for plane stress, and $E'=E/(1-\nu^2)$ for plane strain. By using the beam theory and by taking into consideration the energy due to the transverse shear as well as the bending stresses, for the specimen shown in Fig. 2 the stress intensity factor may be estimated as follows:

$$k_1(b) = P\left(\frac{12}{\pi h_o}\right)^{\frac{1}{2}} \sqrt{F} \tag{38}$$

where the shape factor is calculated to be

$$F = \frac{L^2}{h_o^2} + \frac{1+\nu}{5} \tag{39}$$

for $\theta=0$ and

$$F = \frac{h_o}{h_o+L\tan\theta}\left(\frac{1+\nu}{5} + \frac{1}{\tan^2\theta}\right) - \frac{h_o^2(h_o+2L\tan\theta)}{\tan^2\theta(h_o+L\tan\theta)^3} \tag{40}$$

for $\theta>0$ (Fig. 2). A limited comparison of the stress intensity factors obtained from the elasticity and the beam theories is shown in Table 6. Considering the simplicity of the beam solution, one may observe that the agreement between the two results is fairly good. However, one may also observe that the beam theory gives consistently smaller values than that obtained from the elasticity solution. Physically, this is not really surprising. As Fig. 2 indicates, the constraint of the actual specimen is less than that of the pair of cantilever beams. Consequently an end condition which is more realistic than the built-in end of a cantilever beam would give a greater stress intensity factor.

References

1. J.C. Newman, Jr. "An Improved Method of Collocation for the Stress Analysis of Cracked Plates with Various Shaped Boundaries", NASA-TN-D6376 (1971).

2. G.C. Sih, Methods of Analysis and Solutions of Crack Problems, Noordhoff, Leyden, (1973).

(References - cont.)

3. M.B. Civelek and F. Erdogan, "Crack Problems for a Rectangular Plate and an Infinite Strip", Int. Journal of Fracture, Vol. 19, pp. 139-159 (1982).

4. N.I. Muskhelishvili, Singular Integral Equations, P. Noordhoff Ltd., Groningen-Holland (1953).

5. G.D. Gupta and F. Erdogan, "The Problem of Edge Cracks in an Infinite Strip", Journal of Appl. Mech., Vol. 41, Trans. ASME, pp. 1001-1005 (1974).

6. F. Erdogan, "Mixed Boundary Value Problems in Mechanics", Mechanics Today, Vol. 4, S. Nemat-Nasser, ed., pp. 1-86 Pergamon Press, Inc. (1978).

Acknowledgement. This work was supported by NASA-Langley under the Grant NGR 39-007-011 and by NSF under the Grant MEA-8414477 and was completed when the second author was an Alexander von Humboldt Senior U.S. Scientist Awardee in Freiburg (i. Br.), Germany.

Table 1. Modes I and II normalized stress intensity factors in a long strip under uniform tension σ_0 which contains two symmetrically located inclined edge cracks, B/H = 0.2, c=0, a=b (Fig. 3).

	θ	ℓ/H					
		0.1	0.2	0.3	0.4	0.5	0.6
$\frac{k_1(d)}{\sigma_0\sqrt{\ell}}$	0°	1.1101	1.2123	1.4693	1.8967	2.5980	3.8235
	5°	1.1149	1.2343	1.5071	1.9576	2.6960	3.9936
	10°	1.1058	1.2358	1.5128	1.9647	2.7002	3.9974
	15°	1.0831	1.2169	1.4870	1.9210	2.6201	3.8559
	30°	0.9408	1.0521	1.2531	1.5591	2.0314	2.8337
$\frac{k_2(d)}{\sigma_0\sqrt{\ell}}$	0°	-0.0323	-0.1083	-0.1694	-0.2280	-0.2937	-0.3597
	5°	0.0319	-0.0266	-0.0642	-0.0854	-0.0880	-0.0463
	10°	0.0953	0.0551	0.0416	0.0526	0.1087	0.2302
	15°	0.1560	0.1333	0.1422	0.1875	0.2822	0.4631
	30°	0.3032	0.3188	0.3697	0.4603	0.6047	0.8460

Table 2. Normalized stress intensity factors in a long strip under uniform tension σ_0 which contains three edge cracks of equal length; B/H = 0.2, c=0, a=0, d=b=ℓ (Fig. 3).

θ	ℓ	$k_1(b)/\sigma_0\sqrt{\ell}$	$k_1(d)/\sigma_0\sqrt{\ell}$	$k_2(d)/\sigma_0\sqrt{\ell}$
0°	0.01	1.1100	1.1149	0.0005
	0.11	0.7923	0.9849	-0.1080
	0.21	0.8311	1.1134	-0.1740
	0.31	0.9929	1.3656	-0.2398
	0.41	1.2902	1.7747	-0.3251
	0.51	1.8205	2.4480	-0.4452
5°	0.01	1.1102	1.1091	0.0592
	0.11	0.8089	0.9987	-0.0485
	0.21	0.8618	1.1394	-0.1031
	0.31	1.0481	1.4080	-0.1462
	0.41	1.3874	1.8432	-0.1950
	0.51	1.9915	2.5624	-0.2485
15°	0.01	1.1112	1.0625	0.1727
	0.11	0.8566	0.9815	0.0745
	0.21	0.9466	1.1265	0.0388
	0.31	1.1886	1.3947	0.0283
	0.41	1.6102	1.8251	0.0355
	0.51	2.3360	2.5372	0.0764
30°	0.01	1.1136	0.9145	0.3049
	0.11	0.9488	0.8573	0.2227
	0.21	1.0913	0.9707	0.2113
	0.31	1.3933	1.1781	0.2393
	0.41	1.8832	1.5011	0.3059
	0.51	2.6784	2.0131	0.4375

Table 3. Normalized stress intensity factor $k_1(b)/\sigma_0\sqrt{\ell}$ in a tapered specimen containing an edge crack and subjected to uniform crack surface pressure (Fig. 1a).

		ℓ/H			
B/H	θ	0.1	0.3	0.5	0.7
0.48	0°	1.2499	1.9275	3.0924	6.4152
	10°	1.2164	1.7748	2.9123	6.3642
	20°	1.2048	1.7212	2.8625	6.3565
	30°	1.1974	1.6930	2.8435	6.3549
0.2	0°	1.6747	4.0862	7.3316	10.7602
	10°	1.5066	2.7726	3.9822	.6.7785
	20°	1.4194	2.2798	3.2527	6.4318
	30°	1.3574	2.0052	2.9977	6.3694

Table 4. Normalized stress intensity factor $k_1(b)/(P\sqrt{\ell}/H)$ in a tapered specimen which contains an edge crack and is subjected to a pair of concentrated forces P, a=0, B/H=0.48, m/H=0.2, n/H=0.32, (Fig. 1b).

	ℓ/H					
θ	0.1	0.2	0.3	0.4	0.5	0.6
0°	2.8736	3.6792	4.5127	5.2761	6.2305	7.8916
10°	2.8067	3.4466	4.1153	4.8043	5.8059	
20°	2.7201	3.3067	3.9374	4.6296	5.6743	

Table 5. Normalized stress intensity factor $k_1(b)/(P\sqrt{\ell}/H)$ in a tapered specimen which contains an edge crack and is subjected to concentrated wedge forces P; a=0, B/H=0.48, m/H=0.2, n=0 (Fig. 1b).

θ	ℓ/H				
	0.3	0.4	0.5	0.6	0.7
0°	5.3245	5.4715	6.2768	7.8647	
10°	4.9568	5.0104	5.8537	7.5822	11.2294
20°	4.8228	4.8608	5.7348	7.5170	11.2130
30°	4.7624	4.7996	5.6917	7.4964	11.2093

Table 6. Comparison of the stress intensity factors $k_1(b)/(P/\sqrt{H})$ calculated from the elasticity solution and from the beam theory for a slender tapered specimen; a=0, B/H=0.1, m/H=0.067, n/H=0.05, ℓ-m=L, (Fig. 2).

θ		L/H			
		0.3	0.4	0.5	0.6
10°	Elasticity	9.70	10.40	11.22	11.85
	Beam	8.31	9.59	10.61	11.37
20°	Elasticity	6.38	6.73	6.89	7.11
	Beam	5.94	6.37	6.61	6.73

APPENDIX A

The Green's functions G_{ij} and H_{ij} for a pair of edge dislocations at the point (X_o,Y_o) in an infinite plane.

$$G_{xx}(X,Y,X_o,Y_o) = \frac{2\mu}{\pi(1+\kappa)} \frac{(X_o-X)[(X_o-X)^2-(Y-Y_o)^2]}{[(X_o-X)^2+(Y-Y_o)^2]^2}, \tag{A1}$$

$$G_{yy}(X,Y,X_o,Y_o) = \frac{2\mu}{\pi(1+\kappa)} \frac{(X_o-X)[3(Y-Y_o)^2+(X_o-X)^2]}{[(X_o-X)^2+(Y-Y_o)^2]^2}, \tag{A2}$$

$$G_{xy}(X,Y,X_o,Y_o) = \frac{2\mu}{\pi(1+\kappa)} \frac{(Y-Y_o)[(Y-Y_o)^2-(X_o-X)^2]}{[(X_o-X)^2+(Y-Y_o)^2]^2}, \tag{A3}$$

$$H_{xx}(X,Y,X_o,Y_o) = \frac{2\mu}{\pi(1+\kappa)} \frac{(Y-Y_o)[(Y-Y_o)^2+3(X_o-X)^2]}{[(X_o-X)^2+(Y-Y_o)^2]^2} \tag{A4}$$

$$H_{yy}(X,Y,X_o,Y_o) = \frac{2\mu}{\pi(1+\kappa)} \frac{(Y-Y_o)[(Y-Y_o)^2-(X_o-X)^2]}{[(X_o-X)^2+(Y-Y_o)^2]^2} \tag{A5}$$

$$H_{xy}(X,Y,X_o,Y_o) = \frac{2\mu}{\pi(1+\kappa)} \frac{(X_o-X)[(X_o-X)^2-(Y-Y_o)^2]}{[(X_o-X)^2+(Y-Y_o)^2]^2} \tag{A6}$$

APPENDIX B

The Green's functions Q_{ij} due to a pair of concentrated forces P acting at the points (m,n) and (m,-n) in an infinite plane.

$$Q_{xx}(x,y,m,n) = \frac{1}{2\pi(1+\kappa)} \left\{ \frac{y-n}{(x-m)^2+(y-n)^2} \left[\kappa - 1 - \frac{4(x-m)^2}{(x-m)^2+(y-n)^2} \right] \right.$$

$$\left. - \frac{y+n}{(x-m)^2+(y+n)^2} \left[\kappa - 1 - \frac{4(x-m)^2}{(x-m)^2+(y+n)^2} \right] \right\} , \qquad (B1)$$

$$Q_{yy}(x,y,m,n) = \frac{1}{2\pi(1+\kappa)} \left\{ \frac{y-n}{(x-m)^2+(y-n)^2} \left[-(\kappa+3) + \frac{4(x-m)^2}{(x-m)^2+(y-n)^2} \right] \right.$$

$$\left. - \frac{y+n}{(x-m)^2+(y+n)^2} \left[-(\kappa+3) + \frac{4(x-m)^2}{(x-m)^2+(y+n)^2} \right] \right\} , \qquad (B2)$$

$$Q_{xy}(x,y,m,n) = \frac{1}{2\pi(1+\kappa)} \left\{ \frac{x-m}{(x-m)^2+(y-n)^2} \left[-(\kappa+3) + \frac{4(x-m)^2}{(x-m)^2+(y-n)^2} \right] \right.$$

$$\left. - \frac{x-m}{(x-m)^2+(y+n)^2} \left[-(\kappa+3) + \frac{4(x-m)^2}{(x-m)^2+(y+n)^2} \right] \right\} . \qquad (B3)$$

APPENDIX C

The functions $A_i(\alpha)$, $(i=1,\ldots,4)$.

$$A_i(\alpha) = \sum_{j=1}^{4} E_{ij}(\alpha)R_j(\alpha) \ , \ (i=1,\ldots,4) \ , \tag{C1}$$

$$R_i(\alpha) = F_i(\alpha) + G_i(\alpha) + H_i(\alpha) + P_i(\alpha) \ , \ (i=1,\ldots,4) \tag{C2}$$

$$F_1(\alpha) = \int_a^b C_{11}(\alpha,t)g_1(t)dt \ ,$$

$$G_1(\alpha) = \int_c^d [C_{12}(\alpha,r_o)g_2(r_o) + C_{12}(\alpha,r_o)\tan\theta g_3(r_o)]\cos\theta dr_o \ ,$$

$$H_1(\alpha) = \int_c^d [C_{13}(\alpha,r_o)g_3(r_o) - C_{13}(\alpha,r_o)\tan\theta g_2(r_o)]\cos\theta dr_o \ ,$$

$$P_1(\alpha) = C_{14}(\alpha)P \ , \tag{C3}$$

$$F_2(\alpha) = \int_a^b C_{21}(\alpha,t)g_1(t)dt \ ,$$

$$G_2(\alpha) = \int_c^d [C_{22}(\alpha,r_o)g_2(r_o) + C_{22}(\alpha,r_o)\tan\theta g_3(r_o)]\cos\theta dr_o \ ,$$

$$H_2(\alpha) = \int_c^d [C_{23}(\alpha,r_o)g_3(r_o) - C_{23}(\alpha,r_o)\tan\theta g_2(r_o)]\cos\theta dr_o \ ,$$

$$P_2(\alpha) = C_{24}(\alpha)P \ , \tag{C4}$$

$$F_3(\alpha) = \int_a^b C_{31}(\alpha,t)g_1(t)dt \ ,$$

$$G_3(\alpha) = \int_c^d [C_{32}(\alpha,r_o)g_2(r_o) + C_{32}(\alpha,r_o)\tan\theta g_3(r_o)]\cos\theta dr_o \ ,$$

$$H_3(\alpha) = \int_c^d [C_{33}(\alpha,r_o)g_3(r_o) - C_{33}(\alpha,r_o)\tan\theta g_2(r_o)]\cos\theta dr_o \ ,$$

$$P_3(\alpha) = C_{34}(\alpha)P \ , \qquad \text{(C5)}$$

$$F_4(\alpha) = \int_a^b C_{41}(\alpha,t)g_1(t)dt \ ,$$

$$G_4(\alpha) = \int_c^d [C_{42}(\alpha,r_o)g_2(r_o) + C_{42}(\alpha,r_o)\tan\theta g_3(r_o)]\cos\theta dr_o \ ,$$

$$H_4(\alpha) = \int_c^d [C_{43}(\alpha,r_o)g_3(r_o) - C_{43}(\alpha,r_o)\tan\theta g_2(r_o)]\cos\theta dr_o \ ,$$

$$P_4(\alpha) = C_{44}(\alpha)P \ , \qquad \text{(C6)}$$

$$C_{11}(\alpha,t) = -\frac{1}{\kappa+1}\alpha t\, e^{-\alpha t} \ ,$$

$$C_{12}(\alpha,r_o) = -\frac{1}{\kappa+1}(\alpha x_o e^{-\alpha x_o}\cos\alpha y_o) \ ,$$

$$C_{13}(\alpha,r_o) = \frac{1}{\kappa+1} e^{-\alpha x_o}(\alpha x_o+1)\sin\alpha y_o \ ,$$

$$C_{14}(\alpha) = \frac{1}{4\mu(\kappa+1)} e^{-\alpha m}(\kappa-1-2\alpha m)\sin\alpha n \ , \qquad \text{(C7)}$$

$$C_{21}(\alpha,t) = -\frac{1}{\kappa+1} e^{-\alpha t}(1-\alpha t) ,$$

$$C_{22}(\alpha,r_o) = -\frac{1}{\kappa+1} e^{-\alpha x_o} (1-\alpha x_o)\cos\alpha y_o ,$$

$$C_{23}(\alpha,r_o) = -\frac{1}{\kappa+1} \alpha x_o e^{-\alpha x_o} \sin\alpha y_o ,$$

$$C_{24}(\alpha) = \frac{1}{4\mu(\kappa+1)} e^{-\alpha m}(-\kappa-1+2\alpha m)\sin\alpha n , \qquad (C8)$$

$$C_{31}(\alpha,t) = -\frac{1}{\kappa+1} \alpha(t-H)e^{-\alpha(H-t)} ,$$

$$C_{32}(\alpha,r_o) = -\frac{1}{\kappa+1} \alpha(x_o -H)e^{-\alpha(H-x_o)} \cos\alpha y_o ,$$

$$C_{33}(\alpha,r_o) = \frac{1}{\kappa+1} e^{-\alpha(H-x_o)}[\alpha(H-x_o)+1]\sin\alpha y_o ,$$

$$C_{34}(\alpha) = \frac{1}{4\mu(\kappa+1)} e^{-\alpha(H-m)} \kappa-1-2\alpha(H-m) \sin\alpha n , \qquad (C9)$$

$$C_{41}(\alpha,t) = -\frac{1}{\kappa+1} e^{-\alpha(H-t)}[1-\alpha(H-t)] ,$$

$$C_{42}(\alpha,r_o) = -\frac{1}{\kappa+1} e^{-\alpha(H-x_o)}[1-\alpha(H-x_o)]\cos\alpha y_o ,$$

$$C_{43}(\alpha,r_o) = -\frac{1}{\kappa+1} \alpha(x_o-H)e^{-\alpha(H-x_o)} \sin\alpha y_o ,$$

$$C_{44}(\alpha) = \frac{1}{4\mu(\kappa+1)} e^{-\alpha(H-m)}[\kappa+1-2\alpha(H-m)]\sin\alpha n , \qquad (C10)$$

$$x_o = r_o\cos\theta , \; y_o = B + r_o\sin\theta \qquad (C11)$$

$$E_{11}(\alpha) = (2\alpha D^{-1})[4\alpha^2H^2-(\kappa-1)(-e^{2\alpha H}-2\alpha H+1)] ,$$

$$E_{12}(\alpha) = (2\alpha D^{-1})[4\alpha^2H^2-(\kappa+1)(e^{2\alpha H}-2\alpha H-1)] ,$$

$$E_{13}(\alpha) = (2\alpha D^{-1})[(1-\kappa)(e^{\alpha H}-e^{-\alpha H}) + 2\alpha H(e^{-\alpha H}-\kappa e^{\alpha H})] ,$$

$$E_{14}(\alpha) = (2\alpha D^{-1})[(1+\kappa)(e^{\alpha H}-e^{-\alpha H})-2\alpha H(e^{-\alpha H}+\kappa e^{\alpha H})] , \qquad (C12)$$

$$E_{21}(\alpha) = D^{-1}(-e^{2\alpha H}-2\alpha H+1) ,$$

$$E_{22}(\alpha) = D^{-1}(e^{2\alpha H}-2\alpha H-1) ,$$

$$E_{23}(\alpha) = D^{-1}(2\alpha He^{\alpha H}+e^{\alpha H}-e^{-\alpha H}) ,$$

$$E_{24}(\alpha) = D^{-1}(2\alpha He^{\alpha H}-e^{\alpha H}+e^{-\alpha H}) , \qquad (C13)$$

$$E_{31}(\alpha) = (2\alpha D^{-1})[4\alpha^2H^2+(\kappa-1)(e^{-2\alpha H}-2\alpha H-1)] ,$$

$$E_{32}(\alpha) = (2\alpha D^{-1})[(\kappa+1)(e^{-2\alpha H}+2\alpha H-1)-4\alpha^2H^2] ,$$

$$E_{33}(\alpha) = (2\alpha D^{-1})[(\kappa-1)(e^{\alpha H}-e^{-\alpha H})+2\alpha H(\kappa e^{-\alpha H}-e^{\alpha H})] ,$$

$$E_{34}(\alpha) = (2\alpha D^{-1})[(\kappa+1)(e^{\alpha H}-e^{-\alpha H})-2\alpha H(\kappa e^{-\alpha H}+e^{\alpha H})] , \qquad (C14)$$

$$E_{41}(\alpha) = D^{-1}(e^{-2\alpha H}-2\alpha H-1) ,$$

$$E_{42}(\alpha) = D^{-1}(e^{-2\alpha H}+2\alpha H-1) ,$$

$$E_{43}(\alpha) = D^{-1}(e^{\alpha H}-e^{-\alpha H}+2\alpha He^{-\alpha H}) ,$$

$$E_{44}(\alpha) = D^{-1}(e^{\alpha H}-e^{-\alpha H}-2\alpha He^{-\alpha H}) , \qquad (C15)$$

$$D(\alpha) = e^{2\alpha H}+e^{-2\alpha H}-4\alpha^2H^2-2 \qquad (C15)$$

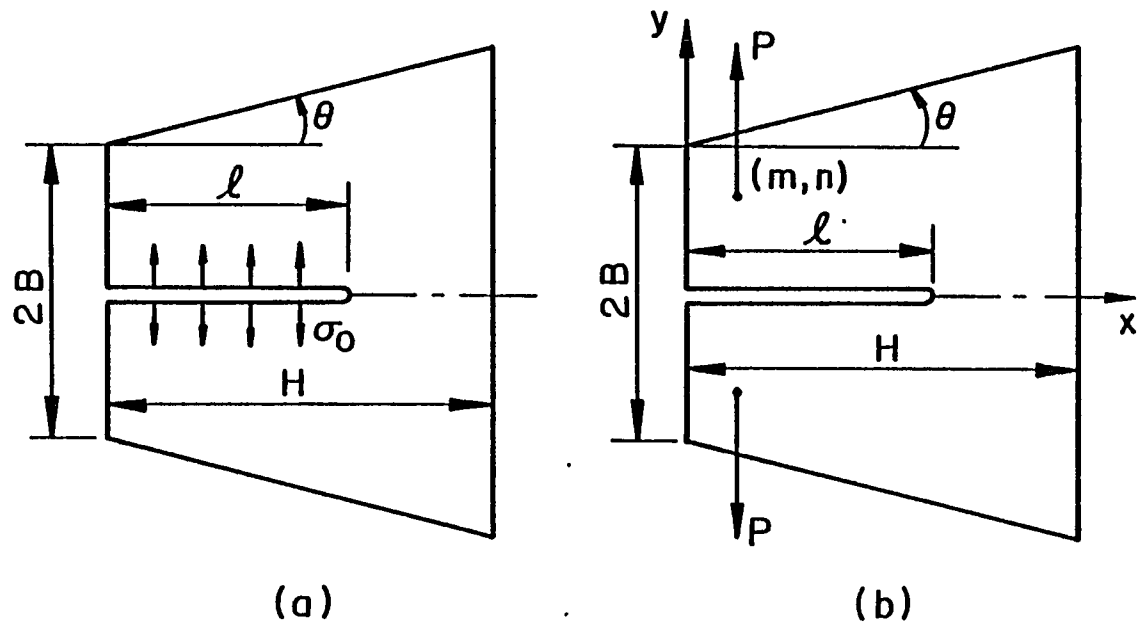

Fig. 1 Geometry and loading conditions for tapered "compact" specimen with an edge crack.

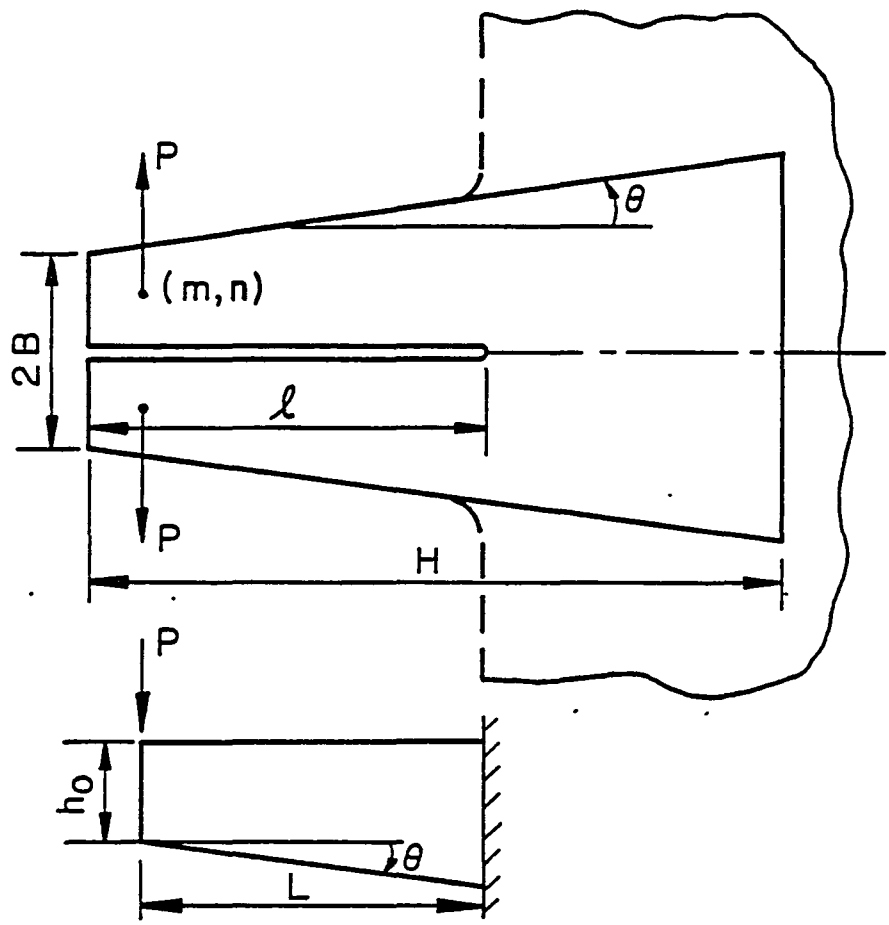

Fig. 2 The tapered "slender" specimen or the tapered double cantilever beam.

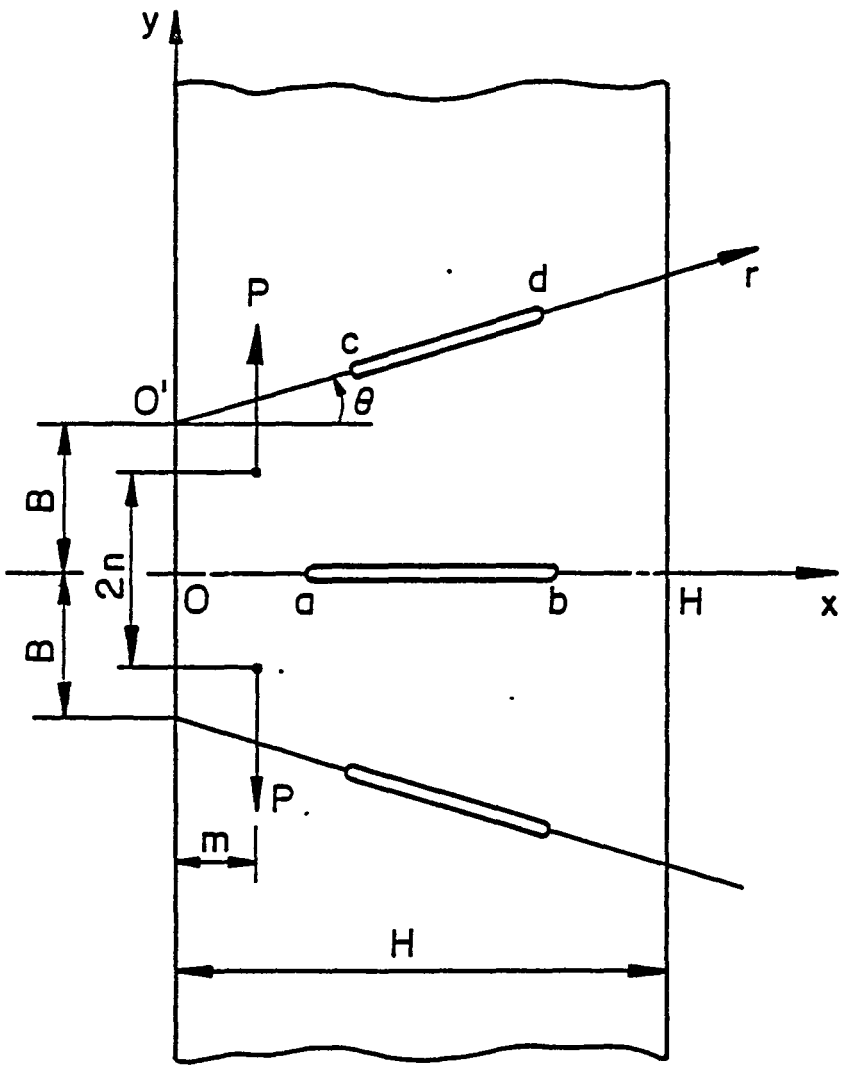

Fig. 3 General description of the inclined crack problem.

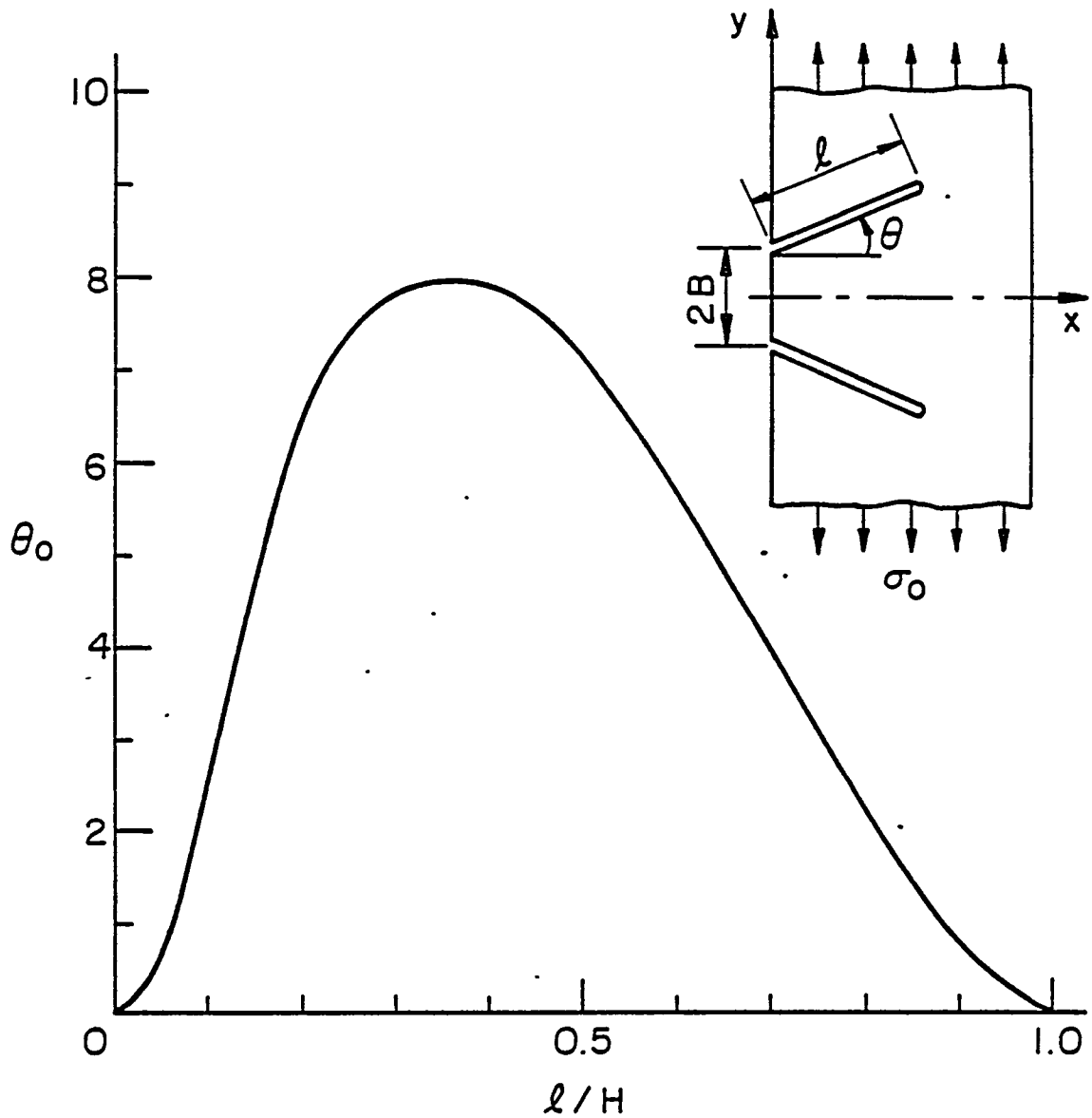

Fig. 4 The angle θ_0 corresponding to zero Mode II stress intensity factor in a long strip containing two inclined edge cracks, B/H = 0.2.

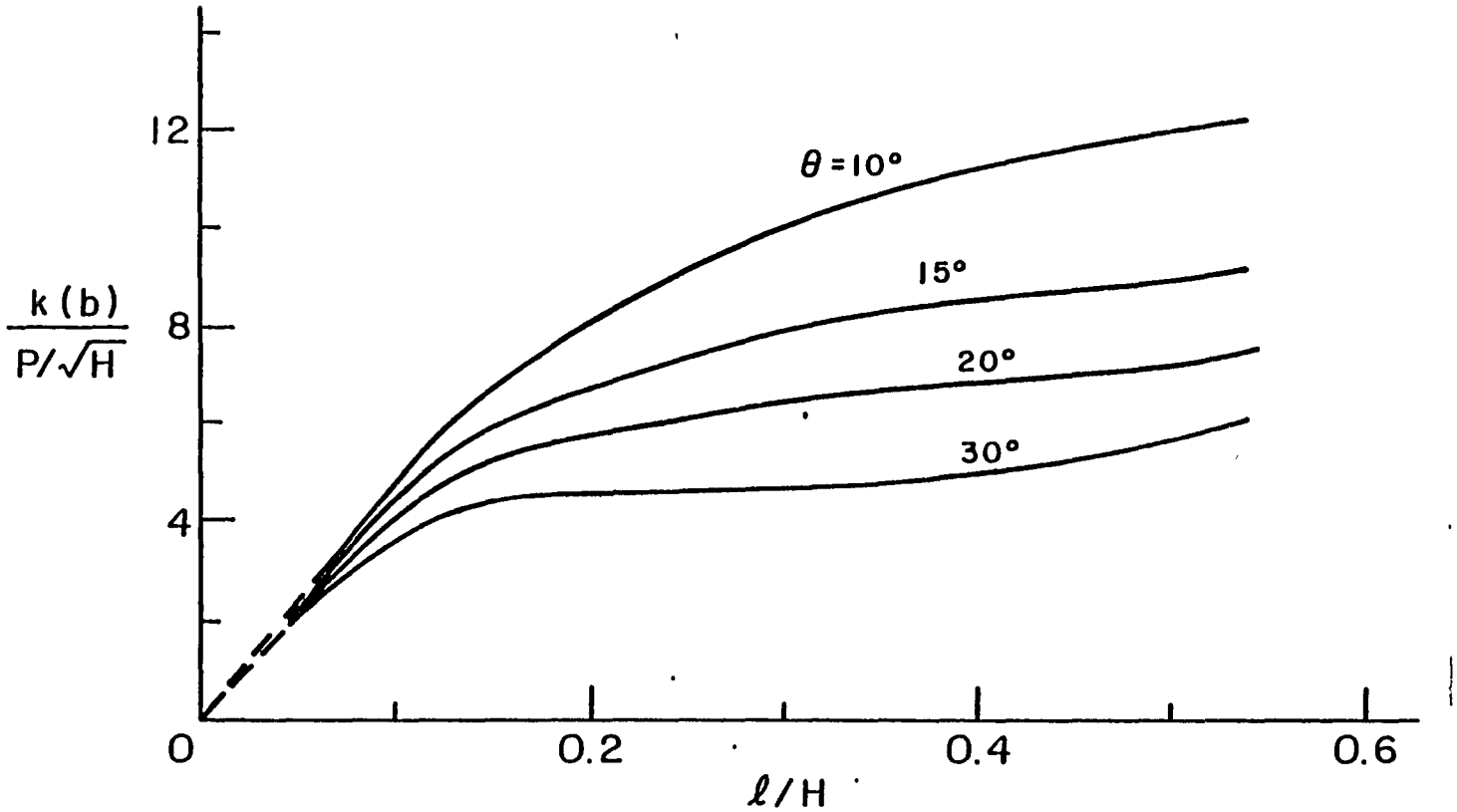

Fig. 5 Stress intensity factor $k_1(b)/(P/\sqrt{H})$ in a "slender" tapered specimen shown in Fig. 2; m/H = 0.067, n/H = 0.05, B/H = 0.1.

1 Report No	2 Government Accession No	3 Recipient's Catalog No
NASA CR-177924		

4 Title and Subtitle	5 Report Date
Stress Intensity Factor in a Tapered Specimen	April 1985
	6 Performing Organization Code

7 Author(s)	8 Performing Organization Report No
Liu Xue-Hui and F. Erdogan	
	10 Work Unit No

9 Performing Organization Name and Address	11 Contract or Grant No
Lehigh University Department of Mechanical Engineering Bethlehem, PA	NGR 39-007-011
	13 Type of Report and Period Covered
12 Sponsoring Agency Name and Address	Contractor Report
National Aeronautics and Space Administration Washington, DC 20546	14 Sponsoring Agency Code
	505-33-23-02

15 Supplementary Notes

Langley Technical Monitor: W. Steven Johnson

16 Abstract

In this paper the general problem of a tapered specimen containing an edge crack is formulated in terms of a system of singular integral equations. The equations are solved and the stress intensity factor is calculated for a "compact" and for a "slender" tapered specimen, the latter simulating the double cantilever beam. The results are obtained primarily for a pair of concentrated forces and for crack surface wedge forces. The stress intensity factors are also obtained for a long strip under uniform tension which contains inclined edge cracks.

17 Key Words (Suggested by Author(s))	18 Distribution Statement
tapered specimen, edge crack, stress intensity factor, double cantilever beam	Unclassified - Unlimited Subject Category 39

19 Security Classif (of this report)	20 Security Classif (of this page)	21 No. of Pages	22 Price*
Unclassified	Unclassified	26	A03

*For sale by the National Technical Information Service, Springfield, Virginia 22151

End of Document